Enhancing Interfacial Toughness in 3D-Printed Soft-Hard Interfaces by Fused Filament Fabrication

UMUT ALTUNTAS, DEMIRKAN COKER
and DENIZHAN YAVAS

ABSTRACT

We proposed a facile strategy for architecting the interface morphology to create tougher and stronger interfaces in additively manufactured multi-material polymer composites in this study. A sutural interfacial morphology between two dissimilar polymer phases PLA (hard) and TPU (soft) is designed and fabricated by the fused filament fabrication technique. The interfacial toughness measurements by the double cantilever beam test reveal a linear correlation between the interfacial toughness and protrusion amplitude. The proposed interfacial architecture can result in up to a 16–18-fold increase in the interfacial toughness in comparison with the baseline interface.

Introduction

Material space has been extending since the beginning of humanity due to requests of engineering applications like high toughness, high strength, high stiffness, and lightness [1]. Now, engineers have a very large material space consisting of natural materials (steel gold), composite materials (alloys, CFRP), and human-made materials (plastic, foam). However, still, there are a lot of empty places in the material space. To create materials that request higher toughness and strength with lightness like aerospace structures, we have to search for a solution in nature [2-4]. Nature gives variable design guidelines to create structures with high strength, high toughness, high impact resistance and lightness through millions of years of evolution [5]. Nature creates a heterogeneous material architecture with dissimilar material by a combination of different microstructures in different length scales. These biological structures have a well-balanced combination of desired properties. The newest method is imitation of the biological structures and to create of bio-inspired structures with a well-balanced combination of desired properties.

These complex bio-inspired structures come with 2 challenges. The first challenge is manufacturing due to their complex geometry and multi-material designs [6]. Traditional methods like injection molding and CNC joining do have not enough capability to fabricate complex multi-material geometries. With recent development in additive manufacturing and material technology, it is possible and affordable to produce complex multi-material geometries with additive manufacturing technologies like fused filament fabrication. FFF 3D printers and their raw materials are relatively cheaper. With dual or more nozzles multi-material parts can be printed. Plastic filament is melted in the printing head and extruded to create desired geometry for FFF method. The second challenge is that force transfers between dissimilar materials through the interface [7]. The interface between dissimilar materials is generally weak due to manufacturing defects and porosities or leaks of chemical adhesion. That causes multi-material structures to tend to fail at their interfaces. Therefore, interface properties of multi-material structures have vital importance to maintain structural rigidity.

*Corresponding Author. dyavas@lamar.edu
Umut Altuntas, Middle East Technical University, No:1 06800 Çankaya Ankara/ TÜRKİYE.
Demirkan Coker, Middle East Technical University, No:1 06800 Çankaya Ankara/ TÜRKİYE.
Denizhan Yavas, Lamar University, 4400 S M L King Jr Pkwy, Beaumont, TX 77705

Architecting the interface morphology is one of the methods to enhance the adhesion between two dissimilar materials. Suture interfaces are one of the most used interface architectures in nature [8-12]. Suture interfaces exhibit wavy or fractal-like hierarchical patterns like triangles, trapezoidal, square waves, and semi-circles. The primary purpose of suture interfaces makes a balance between the strength and flexibility of the biological system while also preserving the integrity of the structure [13]. In addition, sutural interfaces have an important role in toughening mechanisms by mixed-mode fracture due to complex crack growth paths. Because of their advantages, the mechanical and fracture behavior of suture structures is investigated in experimental and numerical by many researchers [8-14]. These researches show that interfacial toughness can be folded by 2-5 times[14]. Recently, the distinctive morphology of sutural interfaces has been utilized to fabricate additively manufactured bioinspired materials or structures with improved mechanical and fracture properties.

In this study, we create change interface morphology between dissimilar soft and hard phases. Suture sutures are introduced to architecting the interface morphology by changing additive manufacturing parameters. We had a detailed investigation of bi-material interface to observe notch effect, adhesive thickness effect and different suture morphology effect. Microscopic examination is made to obtain better correlation between interface properties and real interface architecture. Digital image correlation is used to get traction-separation curves for interfaces.

Method

In this study, the fused filament fabrication method based Ultimaker S5 with dual nozzle 3D printer is used to fabricate multi-material test samples. Printing temperatures are 200°C and 223°C for PLA and TPU , respectively. Printing speeds are 60 mm/s and 25 mm/s for PLA and TPU, respectively. Building bed temperature is set for 60°C to inhibit warpage. PLA is extruded from the left nozzle TPU is extruded from the right nozzle. Layer thickness is 200μm for both materials. CATIA V21 and Cura are used for CAD modeling and slicing, respectively. Fig.1(a) shows the schematic view of the DCB sample and sample orientation. Two PLA adherents stick together with one TPU adhesive. Length of the DCB sample is 118mm and the sample width is 20mm. The thickness of the TPU adhesive is 2mm. The thickness of the PLA adherents is 6mm to keep the beam stiffness high enough and minimize the deformation of PLA adherents. The initial crack length is 28mm, but fracture toughness is calculated after one load-unload cycle according to ASTM-D5528-13. All samples are printed with a 100% infill ratio. The Z-direction is intentionally selected as the printing direction to change interface morphology with the proposed method. Fig. 1(b) shows the interface architecture of sequential layers. PLA and TPU are extruded perpendicular to each other in the same layer. [0°/90°] stack sequence is selected for each side of the interface. This stacking sequence is selected to create enough adhesion between TPU and PLA. The additive manufacturing parameter, overlap distance d, is used to change interface morphology. It changes the penetration

of 90° layers to 0° layers and we can create sutural interfaces. Overlap distance $d = 0, 100, 125, 150, 200\ \mu m$ were used in this study.

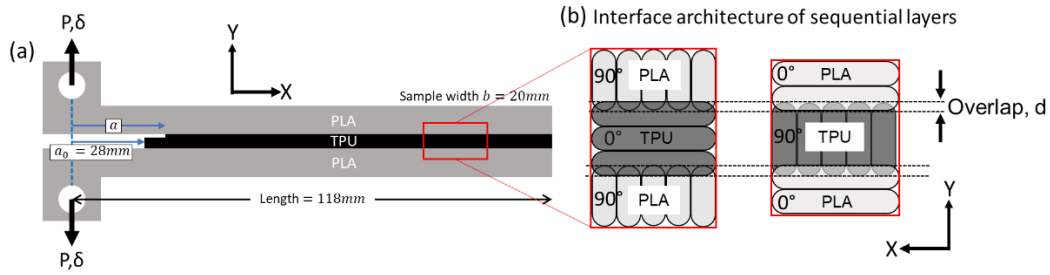

Figure 1 : (a) the schematic view of the DCB sample. (b) the interface architecture of sequential layers

All experiments are performed at 4mm/s displacement control by a universal electromechanical test machine Shimadzu AGS-J with a 10kN load capacity. Force, displacement, and optical images are the output of the experiments. Canon EOS-1D of 5184x3456 pixel with 100mm macro lens is used to take images of samples at 1 Hz during the experiments. Microscopic investigations of all examined interfaces are done by digital microscope Huvitz Company HDS-5800. Small pieces cut from the edge of the DCB samples are used for the characterization of interface morphology. We obtain a better correlation between fracture toughness and real interface morphology by doing this characterization. Examined surfaces are polished with 400, 800, 1200, and 2400 grit polish papers.

Results

Microscopic examination of the interfaces was performed to observe changes in interface morphology with overlap distance d. Fig 2(a) shows the microscope images of examined interfaces on x-y plane for d=0, 150 and 200µm. We can see that protrusion length increases with overlap distance. It is important to mention that there is an asymmetry between the right and left interfaces. In each case, the length of protrusion is higher at the right interface. This suggests that the left interface is weaker, and crack initiation and propagation occur on the left side. Characterization of the left interface is used for a more realistic relationship between the protrusion length and fracture toughness. Also, we observed that interface defect density decreases with overlap distance.

Microscope images are analyzed with IC measure and length of soft protrusion lengths are measured to quantitatively characterize the interface morphology. Fig. 2(b) shows the evaluation of soft protrusion lengths with the increasing overlap distance. For each case, the measurement of protrusion lengths was done in four samples, and at least 20 protrusion lengths were averaged for the reported length.

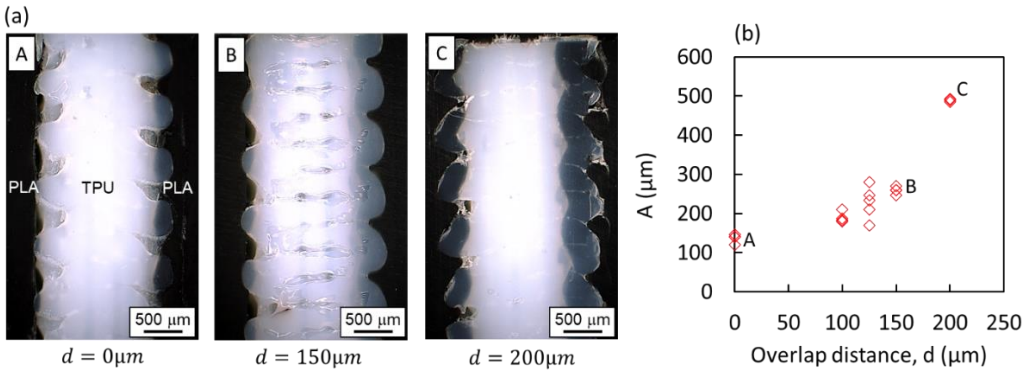

Figure 2: (a) Microscope images of examined interfaces for d = 0, 150, 200µm on xy plane. (b) Protrusion length A as a function overlap distance d.

Fig. 3(a) shows force-displacement curves of DCB samples with different interface morphologies. Each curve slightly softens at the beginning of loading due to the alignment of the fixtures. The weakest interface with A = 140µm has linear deformation with slight non-linearity just before the maximum force. Interfaces with A = 260 and 490 exhibit greater non-linear deformation before the maximum force. The reason might be the larger fracture process zone size at the tip of the crack due to improved interface strength. Maximum load which interfacial crack growth starts increases with protrusion length. Fig. 3(b) shows energy release rate curves for corresponding interfaces as a function of a crack length. It can be said that the energy release rate is enhanced with increasing protrusion length. The weakest interface with A = 140µm has a constant level of energy release rate independent of crack length. It can be suggested that a weak interface shows brittle failure. Interface with A = 260 and 490µm exhibit rising fracture energy release rate with increased crack length. Increased fracture process zone size due to plastic energy dissipation and bridging increase toughness and creates R-curve behavior.

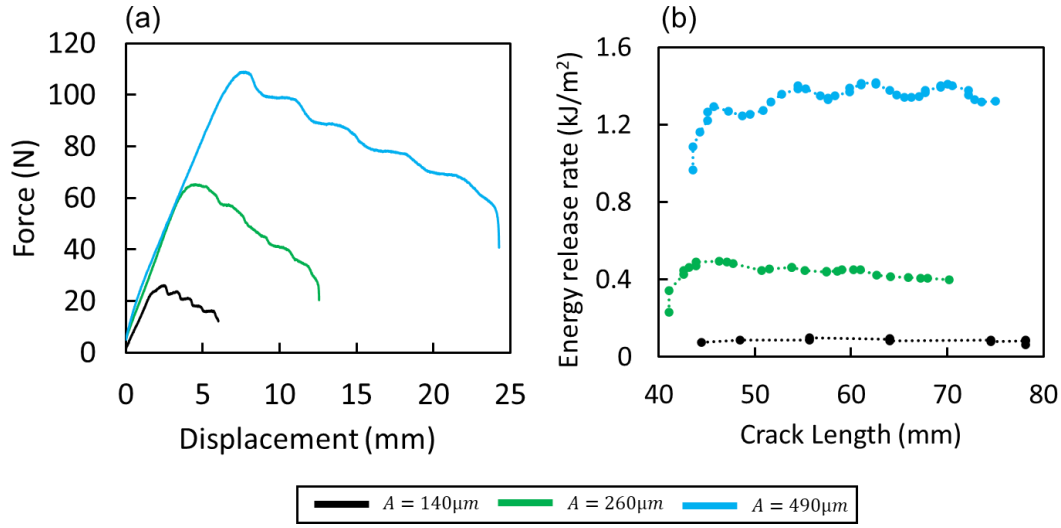

Figure 3: (a) Force-displacement curves for different interface morphologies for DCB test. (b) Corresponding energy release rate curves for different interface morphologies

The initiation G_{in} and steady-state energy release rate G_{ss} can be found in Fig. 3(b). Fig 4(b) shows the variation of G_{ss}/G_{in} as a function of protrusion length. The ratio of G_{ss}/G_{in} is approximately about one for A < 300µm. It is slightly smaller

or larger for a few samples which states rising or decaying R-curve behavior. Exceeding the value of A = 400μm, the ratio of G_{ss}/G_{in} is in the range of 1.5-2. The fracture process zone size increases with increasing crack length due to bridging. The bridging zone can be seen in Fig.4.

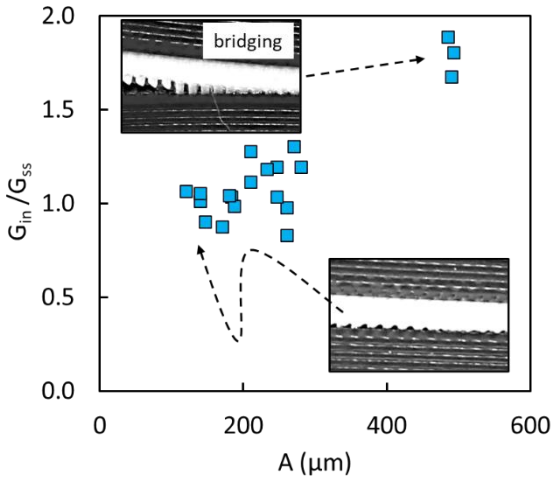

Figure 4: variation on ratio of steady-state energy release rate to initiation energy release rate as a function of protrusion length

To understand better the effect of protrusion length on interface behavior under an opening load, we normalized the initiation and steady-state energy release rate. $(G_{in})_0$ and $(G_{ss})_0$ are the initiation and steady state energy release rate of the weakest interface. G_{in} and G_{ss} are normalized by $(G_{in})_0$ and $(G_{ss})_0$. $(G_{ss})/(G_{ss})_0$ and $(G_{in})/(G_{in})_0$ increase with increasing protrusion length, but $(G_{ss})/(G_{ss})_0$ have a stronger correlation on protrusion length comparison to $(G_{in})/(G_{in})_0$. Each ratio is almost the same for A < 300μm. In that regime, both initiation and steady state energy release rate are increased by 5 times in comparison with the weak interface. Increased real contact area between hard and soft material causes this enchantment. Initiation toughness and steady state toughness for A > 400μm are increased by a factor of 8 and 16 in comparison with the weakest interface, respectively. It can be suggested that plastic energy dissipation due to increased fracture process zone size and bridging toughening mechanism are the reasons for this large enchantment.

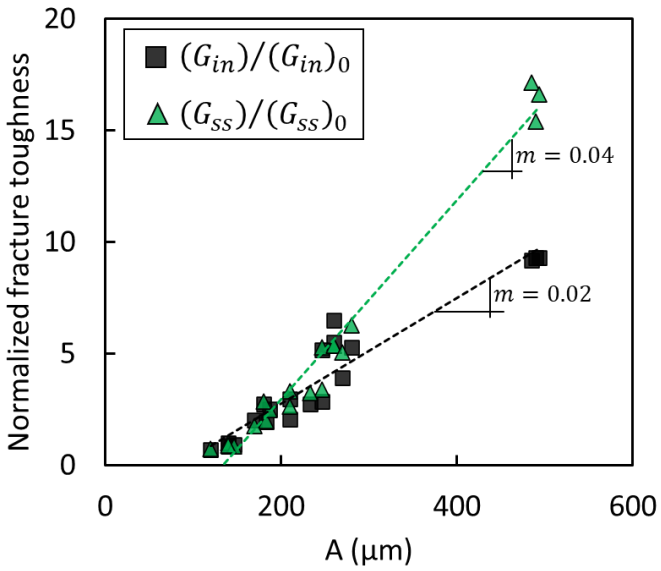

Figure 5 : Normalized fracture toughness of different interfaces

Conclusion

In this study, we proposed a method to change interface morphology with sutural interfaces to increase the fracture toughness of the bi-material interface. Overlap distance one of the additive manufacturing parameters is used to introduce sutural structures to interfaces. The morphology of examined interfaces was quantitively characterized by microscope images. DCB test method is performed to obtain the mode-I fracture behavior of architected interfaces. Results show that the proposed method can change effortlessly interface morphology. The length of soft protrusions increased with increasing overlap distance. The load capacity of the interface and fracture toughness of the interface are enhanced with increased protrusion length. Fracture process zone size and plastic energy dissipation increase with protrusion length, and rising R-curve behavior is observed with increased protrusion length.

REFERENCES

1. Fleck, N. A., Deshpande, V. S., & Ashby, M. F. (2010). Micro-architectured materials: Past, present and future. *Proceedings of the Royal Society A: Mathematical, Physical and Engineering Sciences*, *466*(2121), 2495–2516. https://doi.org/10.1098/rspa.2010.0215
2. Liu J, Li S, Fox K, Tran P. 3D concrete printing of bioinspired Bouligand structure: A study on impact resistance. Additive Manufacturing. 2022 Feb 1;50:102544.
3. Li T, Chen Y, Wang L. Enhanced fracture toughness in architected interpenetrating phase composites by 3D printing. Composites Science and Technology. 2018 Oct 20;167:251-9.
4. Jackson AP, Vincent JF, Turner RM. The mechanical design of nacre. Proceedings of the Royal society of London. Series B. Biological sciences. 1988 Sep 22;234(1277):415-40
5. Ghazlan, A., Ngo, T., Tan, P., Xie, Y. M., Tran, P., & Donough, M. (2021). Inspiration from nature's body armours – a review of biological and bioinspired composites. *Composites Part B: Engineering*, *205*, 108513. https://doi.org/10.1016/j.compositesb.2020.108513
6. Prakash, C., Singh, S., Singh, R., Ramakrishna, S., Pabla, B. S., Puri, S., & Uddin, M. S. (2019). *Biomanufacturing*. Springer International Publishing.
7. D. Yavas, Q. Liu, Z. Zhang, D. Wu, Design and fabrication of architected multimaterial lattices with tunable stiffness, strength, and energy absorption, Mater. Des. (2022), 110613.
8. Liu Z, Zhang Z, Ritchie RO. Interfacial toughening effect of suture structures. Acta Biomaterialia. 2020 Jan 15;102:75-82.
9. Herring SW. Mechanical influences on suture development and patency. Craniofacial sutures. 2008;12:41-56.
10. Cordisco FA, Zavattieri PD, Hector Jr LG, Bower AF. Toughness of a patterned interface between two elastically dissimilar solids. Engineering Fracture Mechanics. 2012 Dec 1;96:192-208
11. Hubbard RP, Melvin JW, Barodawala IT. Flexure of cranial sutures. Journal of biomechanics. 1971 Dec 1;4(6):491-6.
12. Lin E, Li Y, Ortiz C, Boyce MC. 3D printed, bio-inspired prototypes and analytical models for structured suture interfaces with geometrically-tuned deformation and failure behavior. Journal of the Mechanics and Physics of Solids. 2014 Dec 15;73:166-82.
13. R.P. Hubbard, J.W. Melvin, I.T. Barodawala, Flexure of cranial sutures, J. Biomech. 4 (6) (1971) 491–496
14. J. Yin, C. Lu, J. Fu, Y. Huang, Y. Zheng, Interfacial bonding during multi-material fused deposition modeling (FDM) process due to inter-molecular diffusion, Mater. Des. 150 (2018) 104–112